Vortex avalanches in the noncentrosymmetric superconductor Li_2Pt_3B

C. F. Miclea,[1,2,*] A. C. Mota,[1,3] M. Sigrist,[4] F. Steglich,[1] T. A. Sayles,[5] B. J. Taylor,[5] C. A. McElroy,[5] and M. B. Maple[5]

[1]*Max-Planck-Institute for Chemical Physics of Solids, 01187 Dresden, Germany*

[2]*National Institute for Materials Physics, 077125 Bucharest-Magurele, Romania*

[3]*Solid State Laboratory, ETH-Zurich, CH-8093 Zurich, Switzerland*

[4]*Institute for Theoretical Physics, ETH-Zurich, CH-8093 Zurich, Switzerland*

[5]*Department of Physics and Institute for Pure and Applied Physical Sciences, University of California–San Diego, La Jolla, California 92093, USA*

(Received 25 March 2009; revised manuscript received 14 September 2009; published 6 October 2009)

We investigated the vortex dynamics in the noncentrosymmetric superconductor Li_2Pt_3B in the temperature range 0.1–2.8 K. Two different logarithmic creep regimes in the decay of the remanent magnetization from the Bean critical state have been observed. In the first regime, the creep rate is extraordinarily small, indicating the existence of an unconventional very effective pinning mechanism. At a certain time, a vortex avalanche occurs that increases the logarithmic creep rate by a factor of about 5 to 10 depending on the temperature. This may indicate that certain barriers against flux motion are present and they can be opened under increased pressure exerted by the vortices.

DOI: 10.1103/PhysRevB.80.132502 PACS number(s): 74.70.Dd, 74.25.Qt

The occurrence of superconductivity in compounds with noncentrosymmetric crystal structures has attracted considerable attention recently. Besides various other systems, superconductivity has also been reported in the ternary boride compounds Li_2Pd_3B and Li_2Pt_3B which have superconducting critical temperatures of 7–8 K and 2.4 K, respectively.[1,2] These two isostructural compounds crystallize in a structure consisting of distorted boron centered octahedra of BPd_6 or BPt_6 in an approximately cubic arrangement with an interpenetrating lithium sublattice.[3] Both substructures, and hence the composite crystal structure, lack inversion symmetry. Several unusual properties appear in noncentrosymmetric superconductors depending upon various factors, in particular the specific form of the spin-orbit coupling in such systems, as well as the pairing symmetry.[4–6] In contrast to the strongly correlated noncentrosymmetric heavy fermion superconductors $CePt_3Si$,[7] $CeRhSi_3$,[8] and UIr (Ref. 9) for which superconductivity is associated with a magnetic quantum phase transition, there is no evidence of magnetic order or strong electronic correlations in either Li_2Pd_3B or Li_2Pt_3B. Measurements of the London penetration depth suggest that Li_2Pd_3B has a full quasiparticle gap in the superconducting phase, while for Li_2Pt_3B, the data indicate line nodes in the energy gap.[10] NMR measurements[11] suggest that Li_2Pd_3B is a spin singlet, *s*-wave superconductor. In contrast, in Li_2Pt_3B, the spin susceptibility measured by the Knight shift remains unchanged across the superconducting transition temperature, and the spin-lattice relaxation rate $1/T_1$ shows no coherence peak below T_c, decreasing as T^3 with decreasing temperature, consistent with gap line nodes. In this letter, we investigate a further intriguing property of the unconventional superconductor Li_2Pt_3B, observed in the vortex dynamics. We demonstrate that the behavior of the flux creep is very unusual, displaying at short times extremely small creep rates, followed by a faster avalanchelike escape of magnetic flux.

The polycrystalline samples of Li_2Pt_3B used in this experiment were synthesized in an arc furnace utilizing a two-step process similar to that outlined in the work of Badica *et al.*[2] An initial binary sample of BPt_3 was grown using Pt of purity 99.99% and B of purity 99.999%. In the final step of sample growth, an excess amount of Li was added in order to account for losses during arc melting, giving a Li to BPt_3 ratio of 2.2:1. The crystal structure was verified via powder x-ray diffraction measurements. No impurity or binary phases were detected. The sample used for this investigation has been cut and polished into a slab of thickness $t=0.225$ mm.

Prior to the magnetic relaxation measurements, the Li_2Pt_3B sample was characterized by means of measurements of electrical resistivity ρ, magnetization M, and specific heat C. All three measurements yielded a value of the superconducting critical temperature $T_c=3.0$ K. This value is significantly higher than the values reported in the literature, the highest of which is $T_c=2.4$ K.[2] Evidently, the value of T_c is rather sensitive to the composition of the sample, which could be a further indication that Cooper pairing is unconventional in this compound.

The temperature dependence of the specific heat was measured using a quasi-adiabatic heat pulse method in a ^{3}He cryostat, in the temperature range $0.6\ \text{K} \leq T \leq 20\ \text{K}$, and in magnetic fields up to $H \approx 4$ T. The specific heat in the normal state could be described by the expression $C(T)=C_e(T)+C_l(T)$, where $C_e(T)=\gamma T$ is the electronic contribution and $C_l(T)=\beta T^3$ is the lattice term. The best fit to the data yields $\gamma=7.0$ mJ/(mol K^2) for the electronic specific-heat coefficient and $\Theta_D=203$ K for the Debye temperature, in good agreement with the values $\gamma=7.0$ mJ/(mol K^2) and $\Theta_D=228$ K reported by Takeya *et al.*[12] A relatively sharp jump in the specific heat, $\Delta C=15$ mJ/(mol K), was observed at the transition into the superconducting state, yielding a ratio $\Delta C/\gamma T_c=1.2$, larger than the value of 0.8 reported by Takeya *et al.*[12] but smaller than the weak coupling BCS value of 1.43. Below T_c, $C_e(T)$ decreases nearly as T^2 upon decreasing the temperature to $T \approx 0.5 T_c$, consistent with the behavior reported previously[12] and in contrast to the exponential T dependence expected for a BCS superconductor.

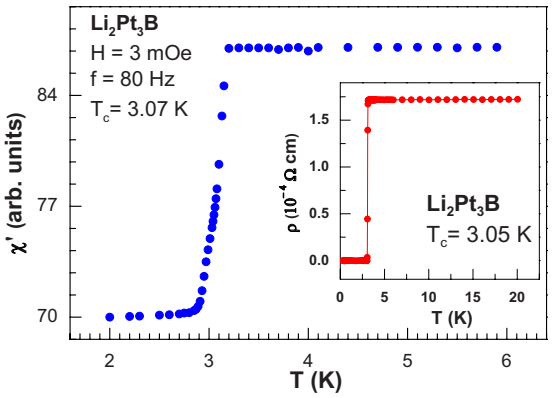

FIG. 1. (Color online) Real part of the ac magnetic susceptibility, χ', as a function of temperature across the superconducting phase transition. Inset: electrical resistivity, ρ, as function of temperature.

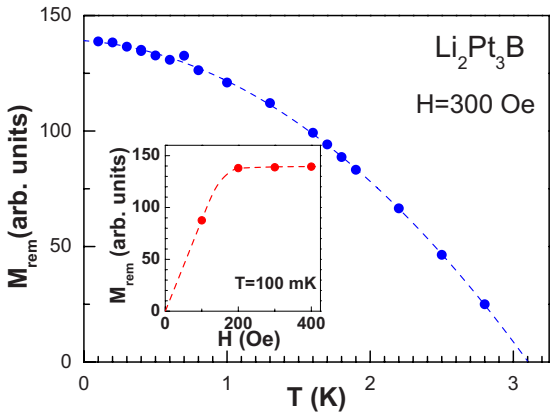

FIG. 2. (Color online) Temperature dependence of the remanent magnetization M_{rem}. The dashed line is a parabolic fit to the data. Inset: M_{rem} as function of the external magnetic field at constant temperature, $T=100$ mK. The dashed line is a guide to the eye.

The upper critical field, H_{c2}, determined from the $C(T)$ measurements, increases linearly with decreasing temperature from T_c to $T=0.6$ K and extrapolates linearly to a value of $H_{c2}(0)\approx 1.5$ T at $T=0$ K.

We also characterized the superconducting transition of the sample by means of ac magnetic susceptibility measurements in a low ac magnetic field of $H=3$ mOe and at a frequency of $f=80$ Hz. This measurement was done with the sample situated inside a custom-built mixing chamber of a dilution refrigerator, using an inductance bridge with a superconducting quantum interference device as a null detector.[13] The midpoint of the superconducting transition of this sample is at $T_c=3.07$ K and the transition width $\Delta T_c=240$ mK. The data are displayed in Fig. 1. In the inset of Fig. 1, we show the low temperature part of the electrical resistivity, $\rho(T)$, measured using a standard four-wire arrangement in a ^{3}He cryostat. $\rho(T)$ displays a sharp phase transition into the superconducting state with a transition width $\Delta T_c=55$ mK and reaches zero at $T=3.05$ K, in very good agreement with the susceptibility data. In the normal state, the $\rho(T)$ measurements revealed typical metallic behavior.

The investigation of vortex dynamics was performed in the temperature range 0.1–2.8 K. Isothermal relaxation curves of the remanent magnetization M_{rem} were taken after cycling the specimen in an external dc magnetic field H. Vortices were introduced into the sample at a slow rate in order to avoid eddy current heating. After waiting for several minutes, the magnetic field was reduced to zero and the relaxation of the metastable magnetization recorded with a digital flux counter for several hours. The sample was prepared in the form of a thin slice, and the magnetic field was applied along the longest direction. At the lowest temperature of our investigation, $T=100$ mK, we determined the field corresponding to the Bean critical state H^*, by estimating the field $H_s(H_s=2\times H^*)$, where the remanent magnetization saturates as function of the external magnetic field. For this sample, we find $H_s=200$ Oe at $T=100$ mK (inset Fig. 2) corresponding to a value of the critical current density $j_c=1.4\times 10^8$ A/m^2. At higher temperatures, the sample will be in the critical state already for smaller external fields as H_s is decreasing upon increasing T. In the main part of Fig. 2, we show values of the remanent magnetization obtained after cycling the sample in a field of $H=300$ Oe as a function of temperature. The remanent magnetization, M_{rem}, decreases monotonically upon increasing the temperature with the experimental data well fitted by a parabola (dashed line in Fig. 2) which reaches zero at around $T\approx 3.1$ K. This is in excellent agreement with the value of T_c yielded by specific heat, ac susceptibility and electrical resistivity measurements.

A typical decay of the remanent magnetization from the critical Bean state at $T=400$ mK is shown in Fig. 3. In this case, the creep was recorded for about 18 000 s. At that time, the sample was heated above T_c in order to obtain the total value of the remanent magnetization as a sum of the amount decayed in the first 18 000 s plus the quantity expelled on crossing T_c. This value is then used to normalize the creep rate. In the inset, the same data are displayed on an expanded scale. We can clearly distinguish two different logarithmic creep regimes. For 50 s$<t<$2400 s, we observe a clear logarithmic relaxation law, with an extremely low relaxation

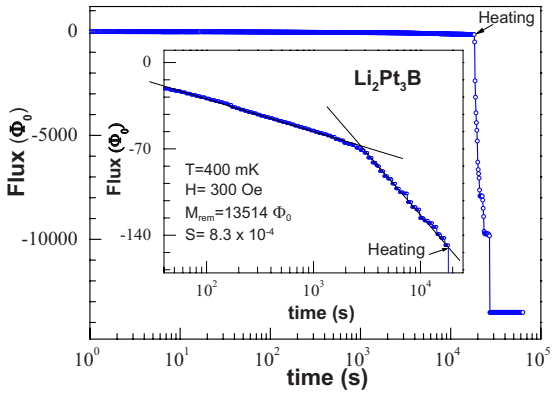

FIG. 3. (Color online) An example of a typical relaxation curve for $T=400$ mK. The magnetic flux is measured as it is expelled out of the sample at constant temperature. After a certain time (marked by arrows in the figure), the sample is gradually heated and driven into the normal state. Inset: Two relaxation regimes are visible in the expanded scale.

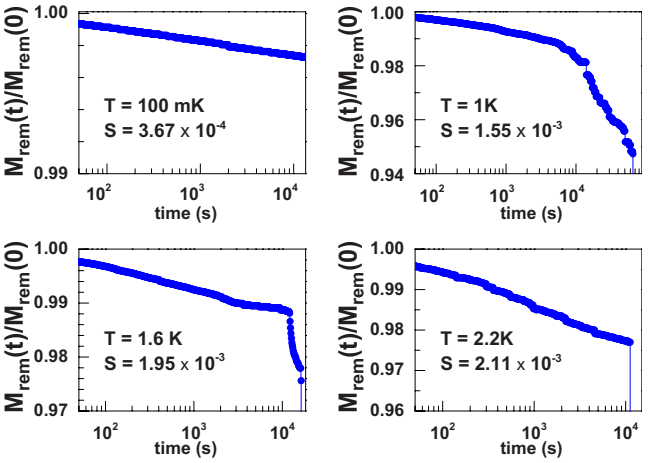

FIG. 4. (Color online) Sequence of isothermal relaxation curves. Two relaxations regimes can be observed at intermediate temperatures as explained in the text.

rate, $S=\partial \ln M/\partial \ln t=8.3\times 10^{-4}$. At around $t=2400$ s, a sudden, strong increase in the relaxation rate occurs, also following a logarithmic law, but with a rate about a factor of four larger, $S=3.1\times 10^{-3}$. Indeed, an avalanchelike escape of vortices has suddenly occurred around $t=2400$ s, indicating that the relaxation process is rather complex. Vortices escaping the sample apparently need a considerable amount of time to overcome a certain barrier. We observed this type of regime change at all temperatures (see Fig. 4), except for relaxations below $T=400$ mK and above $T=2$ K.

To our knowledge, this phenomenon of avalanches in the slow decay of vortices toward equilibrium has never been observed before in any superconductor, conventional or unconventional. This unexpected result points to unconventional vortex physics in this noncentrosymmetric superconductor. The normalized relaxation rates corresponding to the creep before the avalanches occur are depicted in Fig. 5. The upper panel compares, in a double logarithmic plot, the initial slope with the much higher relaxation rate observed during the avalanches. In the lower panel of Fig. 5 we plot the initial relaxation rate in linear scales. These rates are lower by a factor of five even than the very weak creep rates observed in $PrOs_4Sb_{12}$,[14] a superconductor that violates time reversal symmetry. As discussed by Sigrist and Agterberg,[15] the lack of time reversal symmetry in such superconductors allows for the formation of flux-flow barriers formed by fractional vortices on domain walls of the superconductor, that can prevent the motion of normal vortices. It is important to remark that almost the same anomalously weak creep rates as in Li_2Pt_3B have been observed for another noncentrosymmetric superconductor, $CePt_3Si$.[16] However, in CePt3Si no avalanches were detected. The investigated $CePt_3Si$ sample was a high-quality single crystal which showed 13% twinning in single-crystal x-ray diffraction.

We can speculate that the extremely slow motion of flux lines in Li_2Pt_3B could be caused by an unconventional mechanism as recently proposed by Iniotakis *et al.*[17] In many cases for noncentrosymmetric materials, the absence of an inversion center allows for the twinning of the crystal. These authors have shown theoretically that a phase which violates

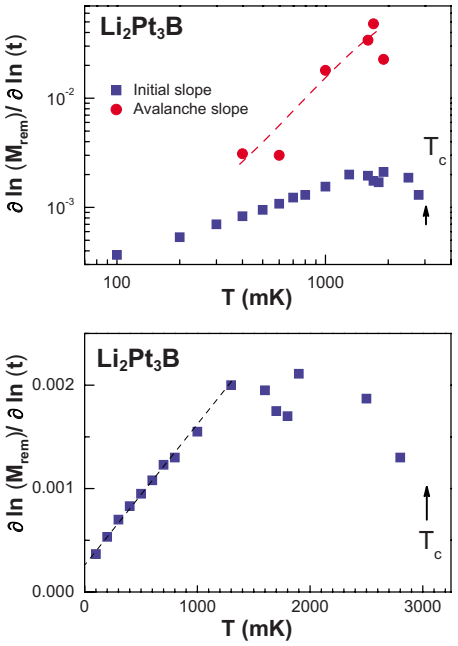

FIG. 5. (Color online) Upper panel: the temperature dependence of the initial decay rate $S=\partial \ln M/\partial \ln t$ together with the relaxation rates observed during the avalanches in a double logarithmic plot. Lower panel: the initial decay rate in a linear plot.

time reversal symmetry can also be realized at interfaces separating crystalline twin domains of opposite spin-orbit coupling. In this case, flux lines with fractional flux quanta could exist on such interfaces and turn twin boundaries into strong barriers impeding flux creep. Within this model, vortex avalanches could be expected when such a fence opens due to excessive pressure of normal vortices. This is possible, if the vortex density increases to a level such that fractional vortices can no longer exist and the vortex pinning mechanism of twin boundaries fails. In the framework of this scenario, we can interpret the temperature window in which the avalanche effect has been observed in the following way. At temperatures below $T=400$ mK, vortices move so slowly that the time necessary to build up the vortex density necessary to break a barrier, exceeds the observation time. For temperatures above $T=2$ K, on the other hand, the overall density of vortices is strongly reduced (see Fig. 2), so that it becomes more difficult to reach the density required for demolishing barriers. However, one cannot rule out other scenarios which would account for the anomalous behavior discovered in this noncentrosymmetric superconductor in the low vortex density regime, namely, the lower vortex creep rates ever observed in spite of a low critical current density, followed by sudden avalanches.

In conclusion, we have observed in Li_2Pt_3B strong avalanches in the relaxation of the remanent magnetization. Prior to the avalanches, vortices move toward equilibrium for several hours with an extraordinary slow creep rate despite the low values of the critical current. This experimental fact indicates that a new type of pinning is effective in this noncentrosymmetric superconductor. This type of pinning is different from the conventional pinning by defects, since it is effective only at low vortex densities. If the density of vor-

tices leaving the sample increases close to the barrier keeping them from moving, an avalanche occurs followed by creep rates that are about 5 to 10 times faster. This type of creep behavior has never been observed before.

We would like to thank C. Iniotakis and S. Fujimoto for helpful discussions. C.F.M. would like to acknowledge the support of the German Research Foundation (DFG) under the auspices of the MI 1171/1-1. A-C.M. and M.S. are grateful for financial support from the Swiss Nationalfonds and the NCCR MaNEP. The work done at the University of California was supported by the U.S. Department of Energy under Grant No. DE FG02-04ER46105.

*miclea@cpfs.mpg.de

[1] K. Togano, P. Badica, Y. Nakamori, S. Orimo, H. Takeya, and K. Hirata, Phys. Rev. Lett. **93**, 247004 (2004).
[2] P. Badica, T. Kondo, and K. Togano, J. Phys. Soc. Jpn. **74**, 1014 (2005).
[3] U. Eibenstein and W. Jung, J. Solid State Chem. **133**, 21 (1997).
[4] L. P. Gor'kov and E. I. Rashba, Phys. Rev. Lett. **87**, 037004 (2001).
[5] P. A. Frigeri, D. F. Agterberg, A. Koga, and M. Sigrist, Phys. Rev. Lett. **92**, 097001 (2004).
[6] V. M. Edelstein, Phys. Rev. B **72**, 172501 (2005).
[7] E. Bauer, G. Hilscher, H. Michor, Ch. Paul, E. W. Scheidt, A. Gribanov, Yu. Seropegin, H. Noël, M. Sigrist, and P. Rogl, Phys. Rev. Lett. **92**, 027003 (2004).
[8] N. Kimura, K. Ito, K. Saitoh, Y. Umeda, H. Aoki, and T. Terashima, Phys. Rev. Lett. **95**, 247004 (2005).
[9] T. Akazawa, H. Hidaka, T. Fujiwara, T. C. Kobayashi, E. Yamamoto, Y. Haga, R. Settai, and Y. Ōnuki, J. Phys.: Condens. Matter **16**, L29 (2004).
[10] H. Q. Yuan, D. F. Agterberg, N. Hayashi, P. Badica, D. Vandervelde, K. Togano, M. Sigrist, and M. B. Salamon, Phys. Rev. Lett. **97**, 017006 (2006).
[11] M. Nishiyama, Y. Inada, and Guo-qing Zheng, Phys. Rev. Lett. **98**, 047002 (2007).
[12] H. Takeya, M. ElMassalami, S. Kasahara, and K. Hirata, Phys. Rev. B **76**, 104506 (2007).
[13] A. Amann, A. C. Mota, M. B. Maple, and H. von Löhneysen, Phys. Rev. B **57**, 3640 (1998).
[14] T. Cichorek *et al.* (unpublished).
[15] M. Sigrist and D. Agterberg, Prog. Theor. Phys. **102**, 965 (1999).
[16] C. F. Miclea, A. C. Mota, M. Nicklas, R. Cardoso, F. Steglich, M. Sigrist, A. Prokofiev, and E. Bauer, arXiv:0904.0257 (unpublished).
[17] C. Iniotakis, S. Fujimoto, and M. Sigrist, J. Phys. Soc. Jpn. **77**, 083701 (2008).